Propagation of elliptic-Gaussian beams in strongly nonlocal nonlinear media

Dongmei Deng and Qi Guo*

Key Laboratory of Photonic Information Technology of Guangdong Higher Education Institutes, South China Normal University,
Guangzhou 510631, People's Republic of China

The propagation of the elliptic-Gaussian beams is studied in strongly nonlocal nonlinear media. The elliptic-Gaussian beams and elliptic-Gaussian vortex beams are obtained analytically and numerically. The patterns of the elegant Ince-Gaussian and the generalized Ince-Gaussian beams are varied periodically when the input power is equal to the critical power. The stability is verified by perturbing the initial beam by noise. By simulating the propagation of the elliptic-Gaussian beams in liquid crystal, we find that when the mode order is not big enough, there exists the quasi-elliptic-Gaussian soliton states.

I. INTRODUCTION

Recently, paraxial optical beams with elliptic geometry, such as standard Ince-Gaussian [1–7], elegant Ince-Gaussian [8], generalized Ince-Gaussian [9], and elliptic [10] beams, which are solutions of the paraxial wave equation in elliptic coordinates, have attracted much attention. The propagation of the optical beams satisfies the nonlocal nonlinear Schrödinger equation [11,12] in the nonlocal nonlinear media. Snyder and Mitchell [11] reduced the nonlocal nonlinear Schrödinger equation (NNLSE) to a linear model named the Snyder-Mitchell model [13] in the strongly nonlocal nonlinear media in 1997. Since then, various types of spatial solitons in highly nonlocal media [14–30] have been studied.

Ince-Gaussian solitons and breathers [17–19] have been studied in strongly nonlocal nonlinear media [11]. Elliptical solitons have also been observed experimentally not only in nonconventionally biased photorefractive crystals [31] but also in nonlinear media with thermal-induced nonlocality [32]. Elliptical solitons in Kerr media have been reported [33,34]. However, the elegant Ince-Gaussian and generalized Ince-Gaussian beams whose patterns are varied periodically have not been explored in nonlinear media.

In this paper, we present a general class of beams called elliptic-Gaussian beams in elliptic coordinates in strongly nonlocal nonlinear media. The Ince-Gaussian solitons and breathers, the elegant Ince-Gaussian, and generalized Ince-Gaussian beams are the special cases of elliptic-Gaussian beams when the distribution factor is taken for some particular values. When the ellipticity parameter tends to infinity or to zero, the elliptic-Gaussian beams change into the self-trapped Cartesian [20] and circular beams [21], respectively. The analytical elliptic-Gaussian beam and elliptic-Gaussian vortex beam solutions of the Snyder-Mitchell model agree well with numerical simulations of the nonlocal nonlinear Schrödinger equation in the case of strong nonlocality. By simulating the propagation of the elliptic-Gaussian beams in the nematic liquid crystal, it is not difficult to find that the quasi-elliptic-Gaussian soliton states can be obtained when the mode order is not big enough.

———————
*Author to whom correspondence should be addressed: guoq@scnu.edu.cn

II. ELLIPTIC-GAUSSIAN BEAMS OF THE SIMPLIFIED MODEL FOR THE NNLSE

The evolution of the $(1 + 2)$-dimensional optical beams in the nonlocal cubic nonlinear media can be described by the nonlocal nonlinear Schrödinger equation [22,23]:

$$i\frac{\partial \Phi}{\partial z} + \mu\left(\frac{\partial^2}{\partial x^2} + \frac{\partial^2}{\partial y^2}\right)\Phi + k\frac{\Delta n}{n_0}\Phi = 0, \qquad (1)$$

where z is the propagation coordinate, $\mu = 1/(2k)$, $k = \omega n_0/c$ is the wave number in the media without nonlinearity, n_0 denotes the linear refractive index of the media, $\Delta n = n_2 \iint_{-\infty}^{\infty} R(\mathbf{r} - \mathbf{r}_1)|\Phi(\mathbf{r}_1, z)|^2 d^2\mathbf{r}_1$ is the nonlinear perturbation of the refraction index, n_2 is the nonlinear index coefficient, $\mathbf{r}$ and $\mathbf{r}_1$ are the two-dimensional transverse coordinate vectors, and R is the normalized symmetrical real nonlinear response function of the media.

In the case of strong nonlocality [11], i.e., when the nonlocal response function is much wider than the beam itself [11,24–26], Eq. (1) simplifies into

$$i\frac{\partial \Phi}{\partial z} + \mu\left(\frac{\partial^2}{\partial x^2} + \frac{\partial^2}{\partial y^2}\right)\Phi - \frac{n_2}{2n_0}k\gamma P_0 r^2 \Phi = 0, \qquad (2)$$

where $r = |\mathbf{r}|$ is the radial coordinate, γ is the material parameter associated with the response function $R(r)$, and P_0 is the input power at $z = 0$. Equation (2) describes the evolution of an optical beam trapped in an effective waveguide structure with the profile given by the nonlocal response function [11,24,25]. Suppose the solution to Eq. (2) can be expressed in terms of

$$\Phi = Z(z)F(u,v)\varphi_G(r,z), \qquad (3)$$

where $u = x/[\sqrt{i}\chi(z)]$, $v = y/[\sqrt{i}\chi(z)]$, and (u,v) are scaled Cartesian coordinates, $\chi(z)$ is a z-dependent scaling factor to be determined, $\varphi_G = \sqrt{P_0}\exp[i\theta(z)]/[\sqrt{\pi}w(z)]\exp\{-r^2/[2w^2(z)] + ic(z)r^2\}$, where $w(z)$ is the beam width of the Gaussian beam, $c(z)$ represents the phase-front curvature of the beam, and $\theta(z)$ is the phase of the complex amplitude. They are given by [27,28], respectively, $w(z) = w_0 (P_c/P_0 \sin^2 \beta_0 z + \cos^2 \beta_0 z)^{1/2}$, $c(z) = k\beta_0 w_0^2(P_c/P_0 - 1)\sin 2\beta_0 z/[4w^2(z)]$, and $\theta(z) = -\arctan(\sqrt{P_c/P_0}\tan\beta_0 z)$, where w_0 is the initial beam width at $z = 0$, $P_c = n_0/(k^2\gamma n_2 w_0^4)$ is the critical power for the soliton propagation, and $\beta_0 = \sqrt{n_2\gamma P_0/n_0}$. Substituting

Eq. (3) into Eq. (2), we obtain the following three differential equations:

$$\frac{d\chi^2}{dz} - 4\mu\chi^2 \left[\frac{i}{w^2(z)} + 2c(z) \right] + 2i\mu = 0, \qquad (4)$$

$$\frac{1}{Z}\frac{dZ}{dz} = \frac{\nu+i}{\chi^2}\mu, \qquad (5)$$

$$\nabla_{u,v}^2 F - \left(u\frac{\partial}{\partial u} + v\frac{\partial}{\partial v} \right) F + (i\nu - 1)F = 0, \qquad (6)$$

where $\nabla_{u,v}^2 = \partial^2/\partial u^2 + \partial^2/\partial v^2$ and ν is a complex separate constant. The solution of Eq. (4) can be expressed as $\chi^2 = \frac{1}{2}w^2(z)\exp[-2i\theta(z)]\{\exp[2i\theta(z)] + C_1\}$, where C_1 is an integral constant. The solution of Eq. (5) is $Z(z) = Z(0)\{\exp[2i\theta(z)] + C_1\}^{(i\nu-1)/2}$, where $Z(0) = (1 + C_1)^{-(i\nu-1)/2}$. Introduce the elliptic coordinate system in the transverse plane perpendicular to z, where the elliptic coordinate [1,35,36] is defined $u = \sqrt{2\epsilon}\cosh\xi\cos\zeta$, $v = \sqrt{2\epsilon}\sinh\xi\sin\zeta$, and $z = z$, ξ and ζ are complex in order to satisfy the requirement that the Cartesian coordinates (x,y) remain real in the entire space, and ϵ is the complex ellipticity parameter. Assuming $F(\xi,\zeta) = M(\xi)N(\zeta)$, Eq. (6) transforms into the Ince equations with complex coefficients [37]

$$\frac{d^2N}{d\zeta^2} + \epsilon\sin 2\zeta\frac{dN}{d\zeta} + [a - \epsilon(i\nu - 1)\cos 2\zeta]N = 0, \qquad (7)$$

$$\frac{d^2M}{d\xi^2} - \epsilon\sinh 2\xi\frac{dM}{d\xi} - [a - \epsilon(i\nu - 1)\cosh 2\xi]M = 0, \qquad (8)$$

where a is a separation constant. Letting $\zeta = i\xi$, Eq. (7) can be transformed into Eq. (8) and vice verse. The solutions of Eq. (7) are given as the generalized Ince function $C_\nu^{(\sigma,m)}(\zeta,\epsilon)$ with degree $m = 0,1,2,\ldots$, parity $\sigma = \{e,o\}$. Rearranging the products of functions of the same parity in ζ and ξ, the general expressions of the even and odd elliptic-Gaussian beams can be expressed as

$$\begin{aligned}
\Phi_\nu^{(\sigma,m)}&(r,\xi,\zeta,\epsilon,z) \\
&= (1 + C_1)^{-(i\nu-1)/2}\{\exp[2i\theta(z)] + C_1\}^{(i\nu-1)/2} \\
&\quad \times \frac{c_\nu^{(\sigma,m)}}{w_0}C_\nu^{(\sigma,m)}(i\xi,\epsilon)C_\nu^{(\sigma,m)}(\zeta,\epsilon)\varphi_G(r,z), \qquad (9)
\end{aligned}$$

where $c_\nu^{(\sigma,m)}$ is the normalization constant, which can be obtained by $\iint_{-\infty}^{\infty}|\Phi_\nu^{(\sigma,m)}|^2 dS = P_0$, where dS is the area differential element across the transverse plane. Equation (9) is the exact solution of Eq. (2). Equation (9) shows that the shape of the even and odd elliptic-Gaussian beams is described by four parameters: ν and m denote a complex continuous radial order and an integer angular mode number, respectively, ϵ is the arbitrarily complex elliptic parameter that determines the ellipticity of the elliptic-Gaussian beams, and the parameter C_1 is the distribution factor that controls the physical size of the beam. When $\nu = -i(p + 1)$ and $p = 0,1,2,\ldots$, Eq. (9) simplifies into elegant Ince-Gaussian beams if $C_1 = 1$, Ince-Gaussian beams, which have been presented in Ref. [19], if $C_1 = 0$, and generalized Ince-Gaussian beams if $C_1 \neq 0,1$. For the case of $\nu \neq -i(p + 1)$, Imν must be less than zero so that the even and odd elliptic-Gaussian beams are square integrable. The transition from the elliptic-Gaussian
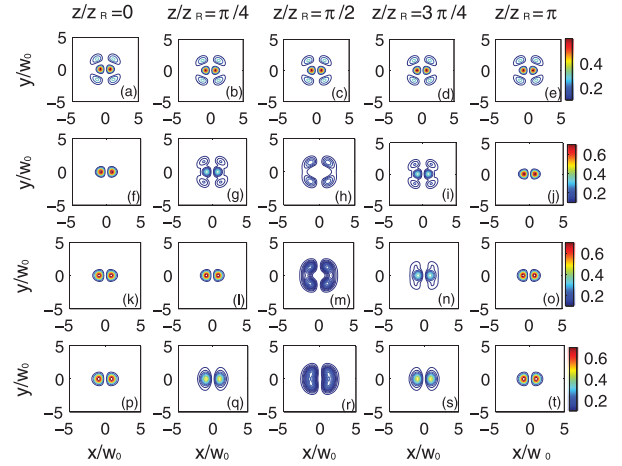
FIG. 1. (Color online) Normalized intensity distribution of the even (3,1)-mode elliptic-Gaussian beams vs x/w_0 and y/w_0 in the different z planes given at the top. The parameters are chosen as $p = 3$, $m = 1$, $P_0/P_c = 1$, $\epsilon = 2$, $z_R = kw_0^2$ is the Rayleigh range, and (a)–(e) $C_1 = 0.0$, (f)–(j) $C_1 = 0.5$, (k)–(o) $C_1 = 1.0$, and (p)–(t) $C_1 = 2.0$.

beams to self-trapped circular beams happens as the elliptical coordinates tend to the cylindrical coordinates, i.e., as $\epsilon \to 0$. On the other hand, the transition from elliptic-Gaussian beams to self-trapped Cartesian beams occurs when $\epsilon \to \infty$.

Equation (9) is a more general family of the solution presented in Ref. [19], i.e., the solution presented in Ref. [19] is the special case of the solution (9) for $\nu = -i(p + 1)$ (where $p = 0,1,2,\ldots$) and $C_1 = 0$. By observing some particular intensity profiles, we can expect that they be distinguished in experiment; e.g., when $P_0 = P_c$, the patterns of the beams vary periodically due to the distribution factor $C_1 \neq 0$, and the patterns of the elliptic-Gaussian solitons ($C_1 = 0$) are stable during propagation.

Figures 1 and 2 show the normalized intensity distribution of the even and odd (3,1)-mode elliptic-Gaussian beams versus x/w_0 and y/w_0. The even and odd elliptic-Gaussian beams are solitons when $P_0/P_c = 1$ and $C_1 = 0$ and are periodic breathers with the period πz_R when $C_1 \neq 0$.

III. ELLIPTIC-GAUSSIAN VORTEX BEAMS OF THE SIMPLIFIED MODEL FOR THE NNLSE

The elliptic-Gaussian vortex beams can be constructed by combining the even- and odd-mode elliptic-Gaussian beams,

$$\Psi_\nu^{\pm,m} = \frac{1}{\sqrt{2}}\left[\Phi_\nu^{(e,m)} \pm i\Phi_\nu^{(o,m)} \right]. \qquad (10)$$

The elliptic-Gaussian vortex beams are the continuous transition modes between the self-trapped Cartesian vortex beams and the self-trapped circular vortex beams when the elliptic parameter ϵ changes continuously. Figure 3 presents the normalized intensity distribution of the elliptic-Gaussian vortex beams versus x/w_0 and y/w_0. When $P_0/P_c = 1$ and $C_1 = 0$, the elliptic-Gaussian vortex beams propagate stably and are vortex solitons; in the case of $C_1 \neq 0$, the elliptic-Gaussian vortex beams vary with the period πz_R during propagation and become a periodic vortex breather.
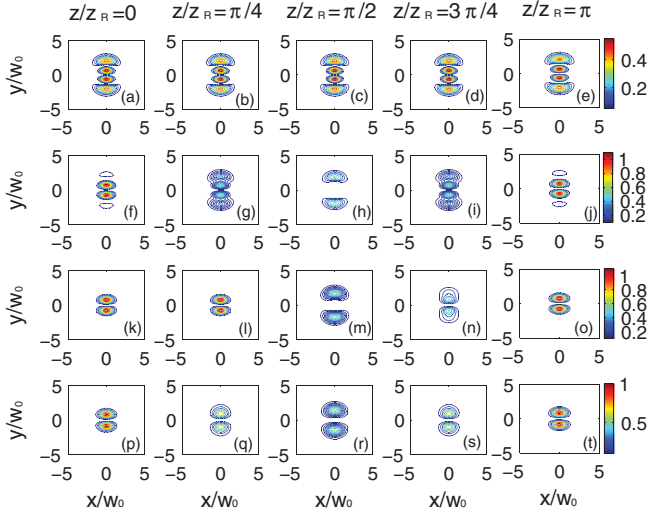
FIG. 2. (Color online) Normalized intensity distribution of the odd (3,1)-mode elliptic-Gaussian beams vs x/w_0 and y/w_0 in the different z planes given at the top. The parameters are the same as those in Fig. 1.

The beam diffraction initially overcomes the beam-induced refraction, and the beam initially gets broad as $P_0 < P_c$, while the beam initially becomes narrow for $P_0 > P_c$; when $P_0 = P_c$, the beam diffraction initially equals the beam-induced refraction, and the patterns of the beams vary periodically due to the distribution factor $C_1 \neq 0$. These are elliptic breathers or elliptic vortex breathers whose widths vibrate or whose patterns vary periodically as they travel in the straight path along the z axis. When $P_0 = P_c$ and $C_1 = 0$, diffraction is exactly balanced by nonlinearity, and these are elliptic solitons or elliptic vortex solitons that preserve their widths and patterns during propagation.
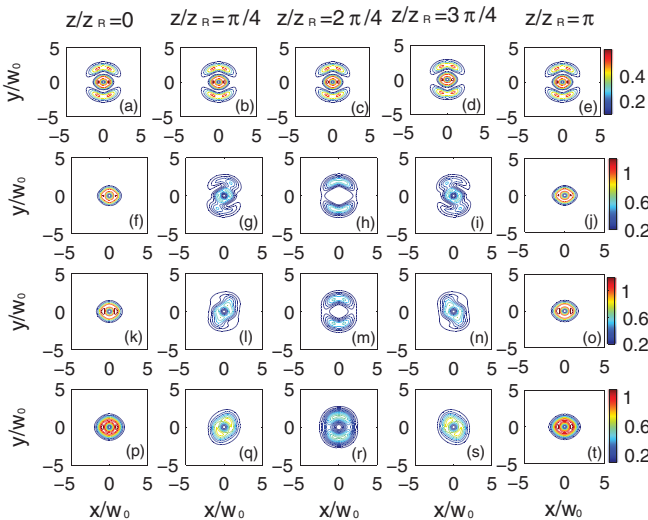
FIG. 3. (Color online) Normalized intensity distribution of the (3,1)-mode elliptic-Gaussian vortex beams vs x/w_0 and y/w_0 in the different z planes given at the top. The parameters are the same as those in Fig. 1.
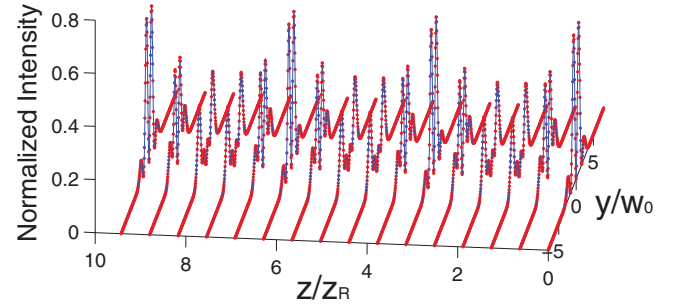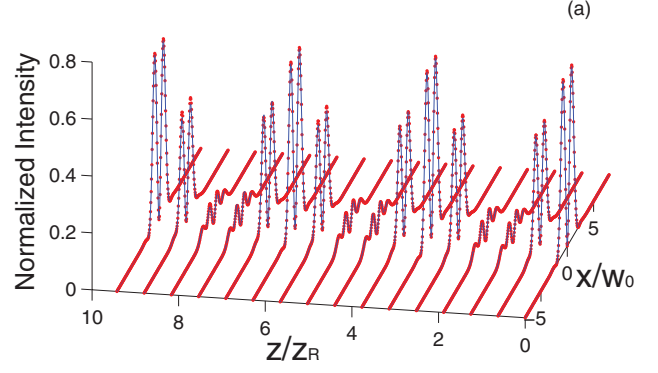
FIG. 4. (Color online) Propagation of the elliptic-Gaussian vortex beams in strongly nonlocal nonlinear media with the Gaussian-shaped response for (a) $x/w_0 = 0$ and (b) $y/w_0 = 0$. The degree of the material nonlocality is $\alpha = 0.01$. The solid line and the dotted line are the numerical solution and the analytical solution, respectively. The parameters are the same as those in Fig. 1(f).

IV. COMPARISON OF THE EXACT ANALYTICAL SOLUTIONS WITH THE EXACT NUMERICAL ONES

Figure 4 shows the comparison of the exact analytical self-trapped elliptic-Gaussian vortex beam solutions for the Snyder-Mitchell model with the exact results of the numerical simulation of Eq. (1) in strongly nonlocal nonlinear media. It is not difficult to find from Fig. 4 that the analytical solutions agree well with the numerical simulations for the case of strong nonlocality. To simulate the propagation, we use the input elliptic-Gaussian vortex beam parameters and suppose the material response to be the Gaussian function [12,24,27,29,30], i.e., $R(r) = 1/(2\pi w_m^2)\exp[-r^2/(2w_m^2)]$, where w_m is the characteristic length of the material response function and $\alpha = w_0/w_m$ is the degree of the material nonlocality, for numerical simulations.

We simulate the propagation of the elliptic-Gaussian beams in a nematic liquid crystal when the material response is assumed to be the zeroth order modified Bessel function of the second kind response material [38–40], i.e., $R(x,y) = 1/(2\pi w_m^2)K_0(\sqrt{x^2 + y^2}/w_m)$. Figure 5 shows the propagation dynamics of the even (3,1)-mode elliptic-Gaussian beams [Figs. 5(a)–5(j)], the odd (3,1)-mode elliptic-Gaussian beams [Figs. 5(k)–(t)], and the (3,1)-mode elliptic-Gaussian vortex beams in the zeroth order modified Bessel function of the
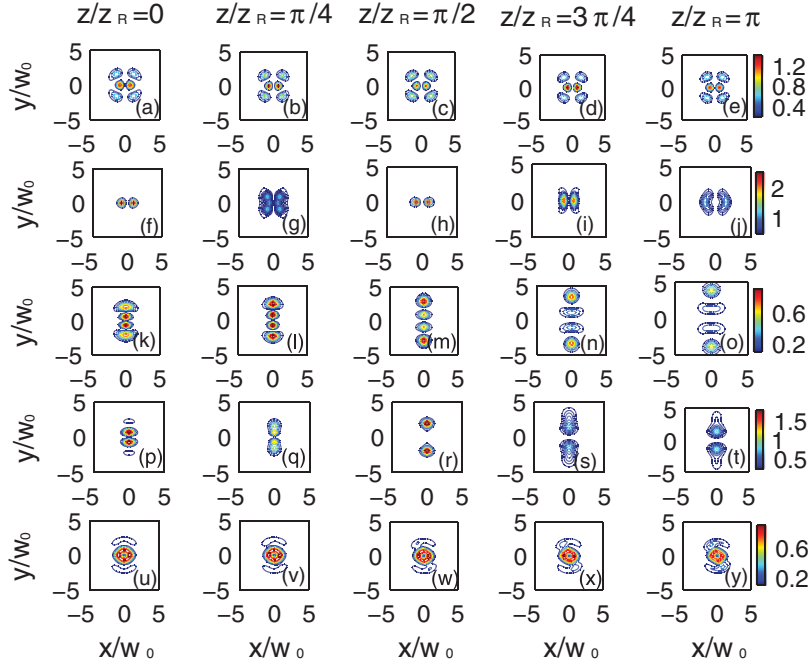
FIG. 5. (Color online) Propagation dynamics of (a)–(j) the even (3,1)-mode elliptic-Gaussian beams, (k)–(t) the odd (3,1)-mode elliptic-Gaussian beams, and (u)–(y) the (3,1)-mode elliptic-Gaussian vortex beams in the zeroth order modified Bessel function of the second kind response material (liquid crystal). The parameters are the same as those in Fig. 1, except $C_1 = 0.0$ in (a)–(e), (k)–(o), and (u)–(y) and $C_1 = 0.5$ in (f)–(j) and (p)–(t).

second kind response material [liquid crystal; Figs. 5(u)–5(y)] with $C_1 = 0.0$ in Figs. 5(a)–5(e), 5(k)–5(o), and 5(u)–5(y) and $C_1 = 0.5$ in Figs. 5(f)–5(j) and 5(p)–5(t). It is easy to find from Fig. 5 that the even (3,1)-mode elliptic-Gaussian beams remain almost stable and become the quasi-elliptic-Gaussian solitons; however, the patterns of the odd (3,1)-mode elliptic-Gaussian beams and the (3,1)-mode elliptic-Gaussian vortex beams change during propagation.

We present the stability analysis of the elliptic-Gaussian beams and elliptic-Gaussian vortex beams by simulating the

FIG. 6. (Color online) Propagation of the elliptic-Gaussian beams and the elliptic-Gaussian vortex beams [(a)–(j) the even (3,1)-mode elliptic-Gaussian beams, (k)–(t) the odd (3,1)-mode elliptic-Gaussian beams, and (u)–(y) the (3,1)-mode elliptic-Gaussian vortex beams] in strongly nonlocal nonlinear media with the Gaussian-shaped response excited by an initial perturbation $\varsigma = 0.05$. The parameters are the same as those in Fig. 5, except the propagation distance $z = 162\pi z_R$.

output normalized intensity distribution of Eq. (1) excited by an initial perturbation. The normalized initial condition is supposed to be $A_0[\Psi(\mathbf{r}) + \varsigma\psi(\mathbf{r})]$, where A_0 is the amplitude of the elliptic-Gaussian beams and elliptic-Gaussian vortex beams, $\Psi(\mathbf{r})$ is the $z = 0$ wave function of the elliptic-Gaussian beams and elliptic-Gaussian vortex beams, $\psi(\mathbf{r})$ is the random complex function whose maximum amplitude is less than 1, and ς denotes the perturbation parameter. Figure 6 shows the propagation of the elliptic-Gaussian beams [Figs. 6(a)–6(j), the even (3,1)-mode elliptic-Gaussian beams; Figs. 6(k)–6(t), the odd (3,1)-mode elliptic-Gaussian beams] and the elliptic-Gaussian vortex beams [Figs. 6(u)–6(y)] in strongly nonlocal nonlinear media with the Gaussian-shaped response excited by an initial perturbation $\varsigma = 0.05$. The parameters are the same as those in Fig. 5 except the propagation distance $z = 162\pi z_R$. The even (3,1)-mode elliptic-Gaussian beams, the odd (3,1)-mode elliptic-Gaussian beams, and the elliptic-Gaussian vortex beams with $C_1 = 0$ propagate unchanged and are stable, and the beam center of the elliptic-Gaussian vortex beams moves during propagation; the even (3,1)-mode elliptic-Gaussian beams with $C_1 = 0.5$ experience periodic variation and are quasistable, and the odd (3,1)-mode elliptic-Gaussian beams with $C_1 = 0.5$ experience strong variations of their profile and are unstable, as is presented in Fig. 6. Stable soliton propagation in numerical experiments where the initial beams is perturbed by noise does not constitute a rigorous proof of stability but does provide strong support for the existence of observable nonlinear modes in laboratory experiments.

V. CONCLUSIONS

In conclusion, we have introduced a general class of elliptic-Gaussian beams and elliptic-Gaussian vortex beams stabilized by the strong nonlocal nonlinearity in elliptic coordinate. The elliptic-Gaussian beams constitute the exact and continuous transition modes between the self-trapped Cartesian and circular beams. The comparisons of analytical solutions of

the Snyder-Mitchell model with numerical simulations of the nonlocal nonlinear Schrödinger equation show that the analytical elliptic-Gaussian beam solutions and elliptic-Gaussian vortex beam solutions agree well with the numerical results in the case of strong nonlocality. In the nematic liquid crystal, the quasi-elliptic-Gaussian soliton states can be obtained.

[1] M. A. Bandres and J. C. Gutíerrez-Vega, Opt. Lett. **29**, 144 (2004).

[2] M. A. Bandres and J. C. Gutíerrez-Vega, J. Opt. Soc. Am. A **21**, 873 (2004).

[3] U. T. Schwarz, M. A. Bandres, and J. C. Gutíerrez-Vega, Opt. Lett. **29**, 1870 (2004).

[4] T. Ohtomo, K. Kamikariya, K. Otsuka, and S. Chu, Opt. Express **15**, 10705 (2007).

[5] S. Chu and K. Otsuka, Appl. Opt. **46**, 7709 (2007).

[6] T. Ohtomo, S. Chu, and K. Otsuka, Opt. Express **16**, 5082 (2008).

[7] J. B. Bentley, J. A. Davis, M. A. Bandres, and J. C. Gutíerrez-Vega, Opt. Lett. **31**, 649 (2006).

[8] M. A. Bandres, Opt. Lett. **29**, 1724 (2004).

[9] M. A. Bandres and J. C. Gutíerrez-Vega, Proc. SPIE **6290**, 62900S (2006).

[10] M. A. Bandres and J. C. Gutíerrez-Vega, Opt. Express **16**, 21087 (2008).

[11] A. W. Snyder and D. J. Mitchell, Science **276**, 1538 (1997).

[12] D. J. Mitchell and A. W. Snyder, J. Opt. Soc. Am. B **16**, 236 (1999).

[13] Y. R. Shen, Science **276**, 1520 (1997).

[14] M. R. Belić and W. P. Zhong, Eur. Phys. J. D **53**, 97 (2009).

[15] W. P. Zhong, M. Belić, T. W. Huang, and R. H. Xie, Eur. Phys. J. D **59**, 301 (2010).

[16] W. P. Zhong and M. Belić, Phys. Lett. A **373**, 296 (2009).

[17] D. M. Deng and Q. Guo, Opt. Lett. **32**, 3206 (2007).

[18] S. Lopez-Aguayo and J. C. Gutiérrez-Vega, Opt. Express **15**, 18326 (2007).

[19] D. M. Deng and Q. Guo, J. Phys. B **41**, 145401 (2008).

[20] D. M. Deng and Q. Guo, Eur. Phys. J. D **60**, 355 (2010).

[21] D. M. Deng and Q. Guo, Opt. Commun. **283**, 3777 (2010).

[22] S. G. Ouyang, W. Hu, and Q. Guo, Phys. Rev. A **76**, 053832 (2007).

[23] W. Hu, S. G. Ouyang, P. B. Yang, Q. Guo, and S. Lan, Phys. Rev. A **77**, 033842 (2008).

[24] W. Krolikowski, O. Bang, J. J. Rasmussen, and J. Wyller, Phys. Rev. E **64**, 016612 (2001).

[25] W. Krolikowski, O. Bang, N. I. Nikolov, D. Neshev, J. Wyller, J. J. Rasmussen, and D. Edmundson, J. Opt. B: Quantum Semiclass. Opt. **6**, S288 (2004).

[26] W. Krolikowski, O. Bang, D. Briedis, A. Dreischuh, D. Edmundson, B. Luther-Daviesa, D. Neshev, N. Nikolov, D. E. Petersen, J. J. Rasmussen, and J. Wyller, Proc. SPIE **5949**, 59490B (2005).

[27] Q. Guo, B. Luo, F. Yi, S. Chi, and Y. Xie, Phys. Rev. E **69**, 016602 (2004).

[28] Q. Guo, Proc. SPIE **5281**, 581 (2004).

[29] A. W. Snyder and Y. Kivshar, J. Opt. Soc. Am. B **11**, 3025 (1997).

[30] W. Krolikowski and O. Bang, Phys. Rev. E **63**, 016610 (2000).

[31] P. Zhang, J. Zhao, C. Lou, X. Tan, Y. Gao, Q. Liu, D. Yang, J. Xu, and Z. Chen, Opt. Express **15**, 536 (2007).

[32] O. Katz, T. Carmon, T. Schwartz, M. Segev, and D. N. Christodoulides, Opt. Lett. **29**, 1248 (2004).

[33] Y. Y. Lin and R. K. Lee, Opt. Lett. **33**, 1377 (2008).

[34] A. S. Desyatnikov, D. Buccoliero, M. R. Dennis, and Y. S. Kivshar, Phys. Rev. Lett. **104**, 053902 (2010).

[35] F. M. Arscott, *Periodic Differential Equations* (Pergamon, Oxford, 1964).

[36] F. M. Arscott, Proc. R. Soc. Edinburgh, Sect. A: Math. Phys. Sci. **67**, 265 (1967).

[37] K. M. Urwin and F. M. Arscott, Proc. R. Soc. Edinburgh, Sect. A: Math. Phys. Sci. **69**, 28 (1970).

[38] G. Assanto and M. Peccianti, IEEE J. Quantum Electron. **39**, 13 (2003).

[39] S. Skupin, O. Bang, D. Edmundson, and W. Krolikowski, Phys. Rev. E **73**, 066603 (2006).

[40] H. Y. Ren, S. G. Ouyang, Q. Guo, W. Hu, and L. G. Cao, J. Opt. A: Pure Appl. Opt. **10**, 025102 (2008).